Evaluating the variation of ion energy under different parameter settings in traveling wave ion mobility mass spectrometry

By: Joseph N. Mwangi, Daniel A. Todd, and Normal H. L. Chiu

Mwangi, Joseph N.; Todd, Daniel A.; Chiu, Norman H.L. (2018). Evaluating the variation of ion energy under different parameter settings in traveling wave ion mobility mass spectrometry. *International Journal for Ion Mobility Spectrometry 21*(3), 81-86. https://doi.org/10.1007/s12127-018-0238-y

This is a post-peer-review, pre-copyedit version of an article published in *International Journal for Ion Mobility Spectrometry*. The final authenticated version is available online at: http://dx.doi.org/10.1007/s12127-018-0238-y.

Abstract:

Ion mobility mass spectrometry (IM-MS) can be used to differentiate and identify isobaric ions. To improve IM-MS resolution, the second generation of traveling wave ion mobility (TWIM) technology was launched. There were reports showing ions were heated up by TWIM. With higher ion energy, it could alter the conformation of larger ions or MS/MS experiments. To monitor the energy exchange relating to the TWIM process, the combined use of thermometer ions with unique molecular structure and theoretical calculations to determine the effective temperature of ions had been explored. In this report, the use of a simple experimental approach to estimate the variation on the ion energy that result from changing a TWIM parameter setting is demonstrated. The approach aims to achieve the same percentage of ion dissociation in a collision cell, which is part of the original instrument and located at the exit of TWIM cell. Similar to the traditional MS/MS experiments, the same level of ion dissociation could be achieved by adjusting the electrical potential that was applied to the collision cell. The higher the ion energy after the TWIM separation, the lower the electrical potential was required to achieve the same level of ion dissociation. Together with the information on the number of electrical charge in the selected ion, the difference in the required electrical potentials could be converted into electron volt of ion energy that resulted from changing the TWIM parameter setting. The results showed ion energy could be changed 1–9 eV when the parameter of TWIM was adjusted.

Keywords: Traveling wave | Ion mobility | Mass spectrometry | Ion heating

Article:

Introduction

The coupling of ion mobility spectrometry to mass spectrometry is considered as a game changer for molecular analysis. The ion mobility spectrometry can provide information on the mobility of

ions in the gas phase, which depends on the mass, charge and shape of ions [1,2,3,4,5,6]. Due to the lack of structural coverage from the ion fragmentation in tandem mass spectrometry, the differentiation of isomeric compounds that may be co-eluted from a chromatography column remain challenging. With the ability to distinguish ions with different molecular shapes, ion mobility spectrometry can be very useful for analyzing structural isomers.

The ion mobility technology that has been coupled to mass spectrometry and commercially available include: drift tube [7, 8], differential ion mobility or high-field asymmetric waveform ion mobility [9], traveling wave [10] and trapped ion mobility [11]. Among the commercialized platforms for ion mobility mass spectrometry (IM-MS), the Waters Synapt series, which bases on the traveling wave technology, has a unique and most versatile instrumental design [12,13,14]. In the Waters Synapt IM-MS instrument, following a switchable ion source, the ions can be sorted out by a quadrupole mass filter before reaching to the setup for traveling wave ion mobility separation. To the best of our knowledge, the Waters Synapt is the only commercialized IM-MS platform that offers the possibility to select molecular ions with specific masses prior to the ion mobility separation. After the ions are transmitted across the traveling wave ion mobility cell, the accurate mass of ions is measured by using an orthogonal time-of-flight mass analyzer. Within the instrumental setup for traveling wave ion mobility separation, it first starts with a trap cell whose primary function is to divide the continuous flow of ions from the quadrupole into batches of ions. Each batch of ions is then analysed in the traveling wave ion mobility cell. Since traveling wave operates under a higher gas pressure than the subsequent time-of-flight mass analyzer, there is a transfer cell at the end of the setup, whose primary function is to transfer ions from the ion mobility cell to the time-of-flight mass analyzer. The unique design of Water Synapt includes making both trap cell and transfer cell to be available for the dissociation of ions. In other words, there are two consecutive collision-induced dissociation (CID) cells, one before the ion mobility cell and one after the ion mobility cell. As a result, there are numerous different ways to utilize the Waters Synapt IM-MS platform.

The drawback of the current ion mobility technology including the traveling wave technology are the lack of sufficient resolving power to distinguish larger ions with similar collision cross sections and the poor rate of ion transmission. In the latter case, one of the possible contributing factors could be the heating of ions inside the ion mobility cell, which may lead to unintended ion dissociation and/or deconformation of larger molecular ions. To address this issue on using the Waters Synapt IM-MS platform, several research groups have attempted to determine the thermal status of ions inside the ion mobility cell. Based on theoretical prediction, Shvartsburg and Smith first reported ion heating in the traveling wave ion mobility separation [13]. De Pauw et al. reported the use of a tailor-made fragile p-methoxybenzylpyridinium as a thermometer ion, and theoretically calculated the effective temperature of ions inside the ion mobility cell [15]. Whereas, Merenbloom et al. reported using a dimeric ion as a probe, and determined most of the ion heating occurred when the ions were injected into the ion mobility cell [16]. Despite the applications of IM-MS have continued to expand, it remains an analytical challenge to investigate the ion energetics in the gas phase during the actual IM-MS measurements. In this report, without using any specific thermometer ions or theoretical calculation, the variation on the ion energy that result from using different parameter settings in traveling wave ion mobility mass spectrometry was estimated.

Materials and methods

Adenosine 3′-monophosphate (AMP)

The AMP ion at 346 m/z was selected as a model precursor ion in this study. AMP was purchased as lyophilized powder with 99% purity (Sigma Aldrich, St. Louis, MO, USA) and was used without any further purification. A stock solution of 1 g/L was prepared by dissolving AMP in autoclaved deionized water and stored at -20 °C. Before the experiments, 10 µM AMP was freshly prepared from the stock solution by using 50:50 H_2O:MeOH as a diluent. For calculating the % dissociation of AMP precursor ion, the fragment ions of PO_3^- at 79 m/z, adenine at 134 m/z, and pentose phosphate at 211 m/z were selected.

Traveling wave ion mobility mass spectrometric measurements

All experimental data was acquired using a Waters Synapt G2 high definition mass spectrometer (Waters, Milford, MA, USA) equipped with an ESI source. The instrument was calibrated using sodium formate solution as recommended by the manufacturer. The sample was delivered by direct infusion at a flowrate of 10 µL/min. The instrument was operated under the MS/MS mobility TOF mode. The source temperature was set 120 °C, the desolvation temperature at 240 °C, the cone gas flowrate was maintained at 50 L/h, and the desolvation gas flowrate at 50 L/h while the other ESI parameters were optimized for an effective ion transmission. Unless otherwise stated, the traveling wave ion mobility cell was operated under the default settings, which included a flow of Argon gas to the trap and transfer cell at 2 mL/min, a flow of Helium gas to the Helium cell at 180 mL/min, a flow of Nitrogen gas to the ion mobility cell at 90 mL/min, wave height at 40 V, and wave velocity at 650 m/s. To minimize the fragmentation of ions in the ion mobility cell, IMS bias voltage was set at 3 V. The TOF mass analyzer was operated under the resolution mode, and the negative ion mode was used. In each experiment, the signals obtained from the sample was acquired for 1 min.

Calculation of % dissociation of precursor ion

The MS/MS spectrum of AMP was retrieved by integrating 1 min time in the ion chromatogram. The ion counts for the precursor ion and the selected fragment ions were used to calculate the percentage of dissociation using the equation below.

$$\%\ \text{dissociation} = \frac{\mathrm{F}}{\mathrm{P} = \mathrm{F}} \times 100$$

where F is the sum of ion counts of selected fragment ions, and P is the ion count of any remaining precursor ion.

No significant hazards or risks are associated with the reported work.

Results and discussion

Different wave height settings

According to the instructions for using the Waters Synapt G2, the key parameters for achieving optimal separation of isomeric or isobaric ions are the wave height and/or wave velocity in the traveling wave ion mobility cell. De Pauw and his associates had reported the vibrational effective temperature of ions inside the traveling wave ion mobility cell went up with increasing wave height [15]. In this report, by allowing ions to pass through the ion mobility cell under the mobility TOF mode and sequentially increase the collision energy in the transfer cell, the extent of ion dissociation (% dissociation) was monitored. As shown in Fig. 1, the % dissociation starts from barely detectable level to increase proportionally with the increasing collision energy being applied to the transfer cell, and eventually levels off at 100% dissociation when excessive collision energy is used. While the parameter settings remain unchanged except the wave height is decreased from the default setting at 40 V, the % dissociation curve of the same precursor ion starts to shift towards the right-hand side in Fig. 1, i.e. higher collision energy is required. This result does comply with the principle of ions surfing and rolling over the traveling wave, thus experience the changes in the wave height [17, 18]. To ensure the positioning of the % dissociation curves in Fig. 1 is reproducible, the same experiment was repeated four times, and the coefficient of variation of each data point was calculated. The average coefficient of variation among the data points in a % dissociation curve was as low as 1.7%. Hence, the error bars of each data point are too small to be effectively shown in Fig. 1. With the Transfer cell located next to the exit of the ion mobility cell, the requirement for using higher collision energy in the transfer cell to achieve the same level of ion dissociation represents the total internal energy of ions was lowered as a result of decreasing the wave height from 40 V. In other words, there is a direct proportional relationship between the total internal energy of ions and wave height. In this study, the total internal energy of ions is defined as the sum of all the rotational, vibrational, kinetic and potential energy of the ions. Without making any changes in the instrumentation or applying any new theoretical calculations for the ion energy, the results of using this rather simple approach to evaluate the ion energy do agree with De Pauw's finding on the relationship between vibrational effective temperature of ions and wave height [15]. In comparison to a report from Williams, the approach in this study uses a precursor ion that is more thermally stable, thus the ion dissociation does not occur until the ions reach the transfer cell [16]. Also, the complete dissociation curve that corresponds to a specific parameter setting is acquired, which then facilitates the comparison of % dissociation under different parameter settings.

The quantitative interpretation of the results in Fig. 1 can provide an estimate on the extents of variation on the total internal energy of ions that resulted from changing the wave height setting. By isolating the linear portion of a % dissociation curve in Fig. 1, and perform a linear regression analysis, the corresponding equation was derived. After working out all the required collision energies to achieve the same level of ion dissociation under the operation of using different wave heights, the differences in the required collision energies are good approximation for the changes in the total internal energy of ions. This is due to the facts that the charge on the ion of interest is known and is equal to one. Plus, the ion collision in the transfer cell is the result of applying the collision energy in voltage to the entrance of the transfer cell, which in turn generates a potential difference between the exit of ion mobility cell and the entrance of transfer cell. When the ions exit from the ion mobility cell, the electrical energy resulting from the potential difference is applied to the ions, which is then converted into the kinetic energy of the ions. While the pressure of Argon gas inside the transfer cell remains constant, the ions collide with the Argon gas and the ion fragmentation is induced. Thus, the difference in the required collision energies

to achieve the same level of ion dissociation under two different wave height settings is a good approximation for the variation on the total internal energy of ions results from changing the wave height. For example, at the level of 50% ion dissociation, changing the wave height from 40 V to 10 V, the total internal energy of the selected precursor ion was calculated to be 9.0 eV lower. The other variations in the total internal energy of ions from changing the wave height are shown in Table 1. This information is applicable for setting up and/or interpreting the results of MS/MS experiments in the mobility TOF mode. In contrast, this information can also be useful to avoid some unwanted conformational change of larger molecular ions or ion fragmentation in the mobility TOF mode by simply lowering the wave height accordingly.

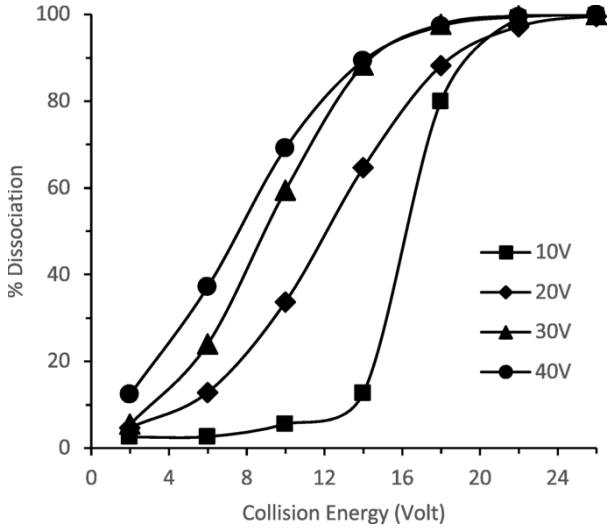

Figure 1. Effects of varying the setting of wave height in voltage (V) in the traveling wave ion mobility cell. The percentage of ion dissociation (% dissociation) is plotted against the collision energy which is being used to induce the ion dissociation in the transfer cell after the precursor ions passing through the traveling wave ion mobility cell. By using the quadrupole located in front of the ion mobility cell, negatively charged ion of AMP with a single charge was selected as precursor ion. The calculation of % dissociation is as described in the "Materials and methods" section. Among the data points, the average CV is ~1.7% (n = 3)

Table 1. Extents of variation of total internal energy of ions in electron volt resulted from changing the wave height between 10 V and 40 V

	10 V	**20 V**	**30 V**	**40 V**
10 V	0.0			
20 V	±4.7	0.0		
30 V	±7.9	±3.2	0.0	
40 V	±9.0	±4.3	±1.1	0.0

The figures shown in the table are estimations at 50% dissociation of precursor AMP ion. The ion energy increases when wave height is increased, and vice versa

Different wave velocity settings

To study the effects of wave velocity on the total internal energy of ions, the wave velocity was either increased or decreased from the default setting of 650 m/s while all the other parameter settings remained constant including the wave height. The results from using wave velocity from

250 m/s to 1050 m/s were acquired and shown in Fig. 2a. When the wave velocity was decreased step-by-step from 1050 m/s, the % dissociation curve of the AMP ion shifts towards higher collision energy, which means more collision energy was required in the transfer cell to achieve the same level of ion dissociation. This, in turn, represents the use of slower wave velocity leads to lower total internal energy in the precursor ions. In other words, there is a direct proportional relationship between the total internal energy of ions and wave velocity.

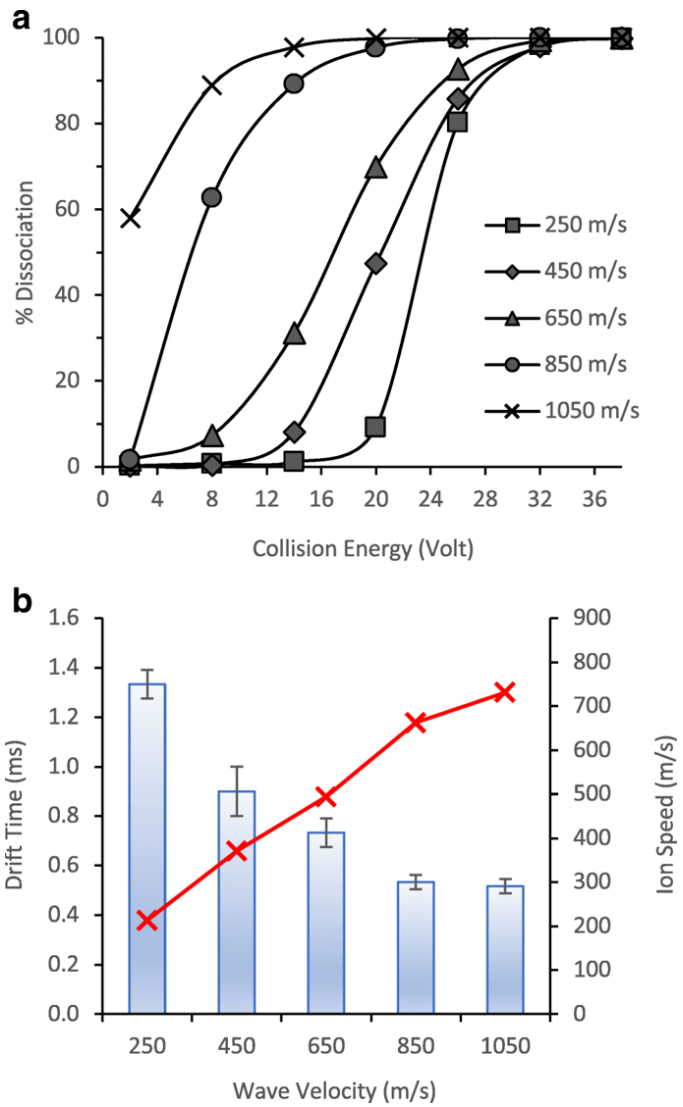

Figure 2. Effects of varying the setting of wave velocity in meter per second (m/s) in the traveling wave ion mobility cell. **a** The percentage of ion dissociation (% dissociation) of precursor AMP ions is plotted against the collision energy being applied to the transfer cell. **b** The bar chart represents the variation of drift time in millisecond (ms) of the precursor AMP ion at different wave velocity. The error bars represent one standard deviation (n = 3). The scatter plot represents the variation of ion speed at different wave velocities. The details for the calculation of ion speed are discussed in the "Results and discussion" section

Since the total internal energy of ions should be directly related to the temperature of ions including its vibrational effective temperature, which as mentioned above was investigated by

De Pauw and his associates. According to De Pauw's finding, there is an inverse proportional relationship between the vibrational effective temperature of ions and wave velocity, i.e. the opposite to what have been observed in Fig. 2a of this study [15]. To further investigate the relationship between the total internal energy of ions and wave velocity, the drift time of the selected AMP precursor ion was measured at different wave velocities. The results are shown in Fig. 2b. The lower the wave velocity, the longer the drift time was measured. These results do comply with the principle of ions surfing and rolling over the traveling wave in the ion mobility cell. If the wave travels at a slower velocity, it would take a longer time for ions to travel across the ion mobility cell. Based on the measured drift time, and approximating the length of the ion mobility cell to be 0.185 m, the ion speed of the precursor ions while traveling across the ion mobility cell with different wave velocities were calculated by using the equation derived by Shvartsburg and Smith as shown below [13].

$$v^2 = 2v_{\mathrm{d(TW)}}\, s^2/\left(s + v_{\mathrm{d(TW)}}\right)$$

where v is the ion speed, s is the wave velocity, $v_{\mathrm{d(TW)}}$ is the drift velocity which is equal to the length of drift cell divide by the drift time of selected ion.

In Fig. 2b, the results of this study show the calculated ion speed increases with increasing wave velocity. As De Pauw and his associates had also pointed out, the ion speed is a good predictor of ion effective temperature [15]. If ion speed goes up with increasing wave velocity, the ion effective temperature should also go up, which in turn increases the total internal energy of ion. Hence, the direct proportional relationship between the total internal energy of ions and wave velocity in Fig. 2a is confirmed. In summary, the results from using the approach of % dissociation curve to evaluate the ion energy do agree with the other finding reported by De Pauw [15].

Buffer gases in ion mobility cell

Based on the principle of traveling wave ion mobility spectrometry, one possible way to further improve the ion mobility separation of ions with very similar collision cross sections is to extend the distance travels by the ions of interest inside the traveling wave ion mobility cell. The longer the travel distance, the higher the resolution on collision cross section. On the other hand, the longer travel distance inside the ion mobility cell could potentially lead to higher level of ion heating. To evaluate the effectiveness of using buffer gas to cool down ions inside the ion mobility cell, the supply of buffer gas to the ion mobility cell was turned off and the extent of ion heating resulted from the absence of buffer gas was evaluated in this study. In the current design, the traveling wave ion mobility cell consists of two parts. At the front of the ion mobility cell, there is a cell filled with Helium buffer gas. The primary function of the Helium cell is to cool down ions prior to the ion mobility separation. In the second half of the ion mobility cell, where ion mobility separation is taken place, the cell is filled with Nitrogen buffer gas. In an initial study, the supply of both buffer gases were turned off, but no signal could be detected. When only one of the two buffer gases was missing in the ion mobility cell, detectable signals corresponded to the selected ion could be resumed. Through the same experimental approach of using the level of ion dissociation after the ions were transmitted through the ion mobility cell, the extent of ion heating without one of the buffer gases was evaluated. The same AMP ion was

selected as precursor ion, and the % dissociation curve obtained by using the default parameter settings with the presence of both buffer gases was considered as a reference (Fig. 3). By repeating the same measurements when either Helium or Nitrogen buffer gas was turned off, two additional % dissociation curves were acquired. The results are shown in Fig. 3. Both additional % dissociation curves are shifted to the left-hand side of the reference plot in Fig. 3. Shifting the % dissociation curve to the left-hand side of the plot means lower collision energy was required to achieve the same level of % dissociation. This represents the ion energy was increased when one of the two buffer gases was absent. In general, this result does comply with the ion heating reported before when traveling wave ion mobility mass spectrometry was used [15, 16]. In comparison to the earlier reports, in which specific thermometer ions were used, the approach of using the level of ion dissociation after the ions are transmitted through the ion mobility cell can be applied to the evaluation of ion heating in a variety of molecular ions. Also, without making any assumption to calculate the effective temperature of ions as reported in the earlier work, it is a direct yet simple approach to evaluate the variation of ion energy. For the proof of concept as described above, the difference between % dissociation curves was used to evaluate the extent of ion heating. To construct each % dissociation curve, multiple data points were acquired that corresponded to the use of different collision energies in the transfer cell. It is, however, possible to estimate the extent of ion heating by using the differences between the percentage of ion dissociation that are obtained under one or two collision energies in the transfer cell. By referring to the horizontal gap between the linear portion of the % dissociation curves that are parallel to each other in Fig. 3, the use of both Helium and Nitrogen buffer gas at the default flowrates had managed to cancel out as much as ~17 eV of heating from the transmission of AMP ions in the current traveling wave ion mobility cell.

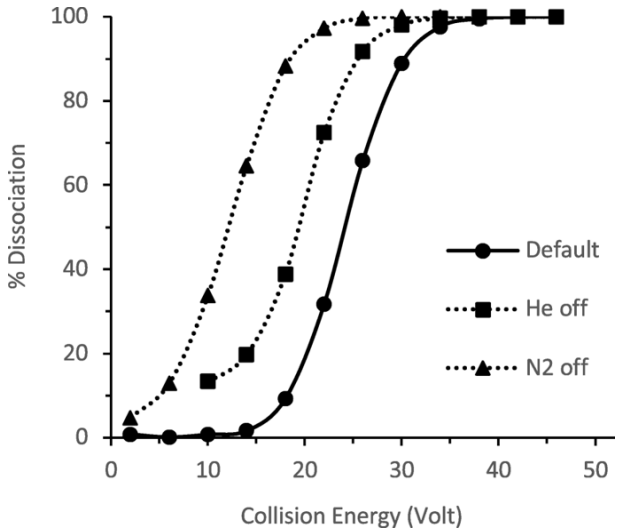

Figure 3. Extent of ion heating without one of the buffer gases in the traveling ion mobility cell. The percentage of ion dissociation (% dissociation) of precursor AMP ions is plotted against the collision energy being applied to the transfer cell. The default curve represents default settings were being used. The He off and N_2 off curves represent the supply of the corresponding gas was turned off

Conclusions

By making use of the unique and versatile design in the Waters Synapt G2 instrument, this report demonstrates the feasibility of using a simple yet practical approach to estimate the variation on the total internal energy of ions which results from using different settings of the key parameters in the traveling wave ion mobility mass spectrometry. There are pros and cons from the results of ion heating when ions are exposed to the traveling wave within the ion mobility cell. If ion dissociation is desirable after the ion mobility separation, the ion heating will be helpful. On the other hand, for the analysis of larger ions, the ion heating may lead to unwanted conformational changes, which will lead to incorrect drift time measurements and sample identification. To control the ion heating in the traveling wave ion mobility cell, the use of both Helium and Nitrogen buffer gas are effective and shown to avoid most of the ion fragmentation. The developed approach can provide a simple way to estimate the changes in ion energy that result from using different parameter settings in traveling wave ion mobility mass spectrometry.

References

1. Dwivedi P, Puzon G, Tam M, Langlais D, Jackson S, Kaplan K, Siems WF, Schultz AJ, Xun L, Woods A, Hill HH (2010) Metabolic profiling of Escherichia coli by ion mobility mass spectrometry with MALDI ion source. J Mass Spectrom 45(12):1383–1393

2. Hofmann J, Hahm HS, Seeberger PH, Pagel K (2015) Identification of carbohydrate anomers using ion mobility-mass spectrometry. Nature 526(7572):241–244

3. Li H, Bendiak B, Siems WF, Gang DR, Hill HH (2015) Determining the isomeric heterogeneity of neutral oligosaccharide-alditols of bovine submaxillary mucin using negative ion traveling wave ion mobility mass spectrometry. Anal Chem 87(4):2228–2235

4. Jeanne Dit Fouque K, Afonso C, Zirah S, Hegemann JD, Zimmermann M, Marahiel MA, Rebuffat S, Lavanant H (2015) Ion mobility-mass spectrometry of lasso peptides: signature of a rotaxane topology. Anal Chem 87(2):1166–1172

5. Allen SJ, Giles K, Gilbert T, Bush MF (2016) Ion mobility mass spectrometry of peptide, protein, and protein complex ions using a radio-frequency confining drift cell. Analyst 141(3):884–891

6. Leijdekkers AG, Huang JH, Bakx EJ, Gruppen H, Schols HA (2016) Identification of novel isomeric pectic oligosaccharides using hydrophilic interaction chromatography coupled to traveling-wave ion mobility mass spectrometry. Carbohydr Res 404:1

7. May JC, Goodwin CR, Lareau NM, Leaptrot KL, Morris CB, Kurulugama RT, Mordehai A, Klein C, Barry W, Darland E, Overney G, Imatani K, Stafford GC, Fjeldsted JC, McLean JA (2017) Conformational ordering of biomolecules in the gas phase: nitrogen collision cross sections measured on a prototype high resolution drift tube ion mobility-mass spectrometer. Anal Chem 86:2107

8. Marchand A, Livet S, Rosu F, Gabelica V (2017) Drift tube ion mobility: how to reconstruct collision cross section distributions from arrival time distributions? Anal Chem 89(23):12674–12681

9. Campbell JL, Le Blanc JC, Kibbey RG (2015) Differential mobility spectrometry: a valuable technology for analyzing challenging biological samples. Bioanalysis 7(7):853–856

10. Zhong Y, Hyung SJ, Ruotolo BT (2011) Characterizing the resolution and accuracy of a second secondgeneration traveling-wave ion mobility separator for biomolecular ions. Analyst 136(17):3534–3541

11. Fernandez-Lima F, Kaplan DA, Suetering J, Park MA (2011) Gas-phase separation using a trapped ion mobility spectrometer. Int J Ion Mobil Spectrom 14(2-3):93–98

12. Giles K, Wildgoose JL, Langridge DJ, Campuzano I (2010) Metabolic profiling of human blood by high resolution Ion Mobility Mass Spectrometry (IM-MS). Int J Mass Spectrom 298(1-3):10–16

13. Shvartsburg AA, Smith RD (2008) Fundamentals of traveling wave ion mobility spectrometry. Anal Chem 80(24):9689–9699

14. D'Atri V, Causon T, Hernandez-Alba O, Mutabazi A, Veuthey JL, Cianferani S, Guillarme D (2018) Adding a new separation dimension to MS and LC-MS: what is the utility of ion mobility spectrometry? J Sep Sci 41(1):20–67

15. Morsa D, Gabelica V, De Pauw E (2011) Effective temperature of ions in traveling wave ion mobility spectrometry. Anal Chem 83(14):5775–5782

16. Merenbloom SI, Flick TG, Williams ER (2012) How hot are your ions in TWAVE ion mobility spectrometry?. J Am Soc Mass Spectrom 23(3):553–562

17. Giles K, Pringle SD, Worthington KR, Little D, Wildgoose JL, Bateman RH (2004) Applications of a travelling wave-based radio-frequency-only stacked ring ion guide. Rapid Commun Mass Spectrom 18(20):2401–2414

18. May JC, McLean JA (2013) The influence of drift gas composition on the separation mechanism in traveling wave ion mobility spectrometry: insight from electrodynamic simulations. Int J Ion Mobil Spectrom 16(2):85–94

Acknowledgements

J.M. wishes to acknowledge the supports received from NSF GK-12 program and Burroughs Wellcome Fund. N.C. wishes to acknowledge the support from an internal research grant. All other financial and technical supports were provided by the Chemistry and Biochemistry Department at UNCG.